Malformations in Late Devonian brachiopods from the western Junggar, NW China and their potential causes

Ruiwen Zong [1], **Yiming Gong** [Corresp. 1]

[1] China University of Geosciences, Wuhan, China

Corresponding Author: Yiming Gong
Email address: ymgong@cug.edu.cn

Although malformations are found in both extant organisms and the fossil record, they are more rarely reported in the fossil record than in living organisms, and the environmental factors causing the malformations are much more difficult to identify for the fossil record. Two athyrid brachiopod taxa from the Upper Devonian Hongguleleng Formation in western Junggar (Xinjiang, NW China) show distinctive shell malformation. Of 198 *Cleiothyridina* and 405 *Crinisarina* specimens, 18 and 39 individuals were ~~deformed~~, respectively; a ~~deformity~~ ~~rate~~ of nearly 10%. Considering the preservation status and buried environment of the ~~deformed~~ specimens, and analysis of trace elements and rare earth elements from whole-rock and brachiopod shells, we conclude that the appearance of deformed athyrids is likely related to epi/endoparasites, or less likely the slightly higher content of heavy metal in the sea.

Malformations in Late Devonian brachiopods from the western Junggar, NW China and their potential causes

Ruiwen Zong, Yiming Gong*

State Key Laboratory of Biogeology and Environmental Geology, and School of Earth Sciences, China University of Geosciences, Wuhan, Hubei, China.

Corresponding Author:

Yiming Gong

Lumo Road No. 388, Wuhan, Hubei, 430074, China

Email address: ymgong@cug.edu.cn

Abstract

Although malformations are found in both extant organisms and the fossil record, they are more rarely reported in the fossil record than in living organisms, and the environmental factors causing the malformations are much more difficult to identify for the fossil record. Two athyrid brachiopod taxa from the Upper Devonian Hongguleleng Formation in western Junggar (Xinjiang, NW China) show distinctive shell malformation. Of 198 *Cleiothyridina* and 405 *Crinisarina* specimens, 18 and 39 individuals were ~~deformed~~, respectively; a ~~deformity rate~~ of nearly 10%. Considering the preservation status and buried environment of the ~~deformed~~ specimens, and analysis of trace elements and rare earth elements from whole-rock and brachiopod shells, we conclude that the appearance of ~~deformed~~ athyrids is likely related to epi/endoparasites, or less likely the slightly higher content of heavy metal in the sea.

Introduction

Deformities are common in living organisms; the term usually refers to soft body or skeletal tissue malformation of individuals that occur during ontogeny. However, malformations are known from the fossil record too, and have been reported from individuals of different fossil groups, including foraminifera (*Ballent & Carignano, 2008*), trilobites (*Owen, 1985; Babcock, 1993*), brachiopods (*Copper, 1967; He et al., 2017*), bivalves (*Savazzi, 1995*), gastropods (*Lindström & Peel, 2010*), cephalopods (*De Baets, Keupp & Klug, 2015; Hoffmann & Keupp, 2015; Mironenko, 2016; De Baets, Hoffmann & Mironenko, 2021*), echinoderms (*Thomka, Malgieri & Brett, 2014*), graptolites (*Han & Chen, 1994*), insects (*Vršanský, Liang & Ren, 2012*), conodonts (*Weddige, 1990*), shark teeth (*Itano, 2013*), amphibians (*Witzmann et al., 2013*),

reptiles (*Buffetaut et al., 2007*), primate teeth (*Tougard & Ducrocq, 1999*), and plankton (*Vandenbroucke et al., 2015; Bralower & Self-Trail, 2016*). In addition to gene mutations or embryonic developmental disorders, deformed fossils may also have resulted from healed injuries and pathology (*Owen, 1985; Babcock, 1993; Kelley Kowalewski & Hansen, 2003; Vinn, 2007, 2008*). Malformed fossils provide important evidence of both organisms-organisms and organisms-environment relationships during geological history. For example, malformed specimens caused by predatory attacks provides us information about the food chain at that time or about the position of prey in the ecological chain (*Kelley Kowalewski & Hansen, 2003*). Moreover, some malformations resulting from diseases or developmental disorders are likely to be related to the habitat of the organism, such as changes in environmental factors, and parasite, viral or bacterial infection (e.g., *Morris, 1981; Rouse, 2005; Vandenbroucke et al., 2015; De Baets et al., 2021*).

Although many malformed fossils have been described, deformed fossils (especially macrofossils) are generally rare, with sometimes only one or two specimens known. Therefore, previous studies have generally been limited to description of deformed specimens and simple classification of the cause(s) of malformation, only in a few cases the relationship between deformed specimens and their habitat has been discussed (*Copper, 1967; Vandenbroucke et al., 2015; Bralower & Self-Trail, 2016; He et al., 2017*). Although many deformed fossils are believed to result from developmental disorders or have pathological causes, the environmental factors responsible for the developmental disorders or diseases are mostly indefinite or speculative. The low number of malformed specimens available often limits further study. The

Upper Devonian succession in western Junggar, Xinjiang, NW China, contains abundant, well-preserved brachiopods. We collected more than 600 athyrid (*Cleiothyridina* and *Crinisarina*) specimens from the Upper Devonian Hongguleleng Formation in the Buninuer section, of which nearly ten percent of individuals were deformed. The aims of current study are to explore the biotic or abiotic stressors of these malformed brachiopods, and the effect of change in environmental factors on the brachiopod shells.

Materials and methods

The material studied in this paper was collected from the Upper Devonian Hongguleleng Formation in western Junggar, Xinjiang. The Hongguleleng Formation is a widely distributed marine unit near the Devonian–Carboniferous boundary in western Junggar. The formation is divided into three members: the Lower Member is composed of thin bioclastic limestones, muddy limestones and shales; the Middle Member is mainly made up of fine pyroclastic rocks with a few sandy and muddy limestones; and the Upper Member consists of calcareous clastic rocks with a small amount of bioclastic limestones (*Hou et al., 1993*). The formation is mostly Famennian in age (*Ma et al., 2017; Zong et al., 2020; Shen et al., 2021; Stachacz et al., 2021*). The Hongguleleng Formation is very rich in many types of the early Famennian fossils, such as acritarchs, bivalves, brachiopods, bryozoans, cephalopods, chondrichthyans, conodonts, conulariids, corals, echinoderms, gastropods, ostracods, plants, radiolarians, spores, trace fossils, and trilobites (*Liao, 2002; and our unpublished specimens*).

Brachiopods occur in all three members of the Hongguleleng Formation. Brachiopod abundance and diversity is highest in the Lower Member, with the groups present including

Productida, Orthida, Rhynchonellida, Athyridida and Spiriferida (*Zong et al., 2016; Zong & Ma, 2018*). Athyrids are most abundant in the Lower Member, with only a few athyrid specimen recovered from the base of the Middle Member and the limestone interlayer of the Upper Member (*Zong et al., 2016*). All the athyrids studied in this paper were extracted from the bioclastic limestone in the upper part of the Lower Member of the Hongguleleng Formation in the Buninuer section, 15 km north of Hoxtolgay town. This section is located about 14 km southwest of the Bulongguoer section, which is the type section of the Hongguleleng Formation (*Hou et al., 1993*). The lithology and fossil assemblages of the Buninuer section are the same as those of the stratotype section, the upper part of the Lower Member of the Hongguleleng Formation of both sections were deposited in a distal storm lithofacies sedimentary environment (*Fan & Gong, 2016*). A total of 603 athyrids in two genera (*Crinisarina* and *Cleiothyridina*) are non-flattened specimens with well-preserved dorsal and ventral valves. Although athyrids occur in other beds of the Hongguleleng Formation, no malformed specimens were found in those levels.

The 603 specimens include a wide range of size and may include individuals representing different growth stages (Supplemental file 1). We divided the shell length (L) into six size classes: 5 mm≤ L< 10 mm; 10 mm≤ L< 15 mm; 15 mm≤ L< 20 mm; 20 mm≤ L< 25 mm; 25 mm≤ L< 30 mm and 30 mm≤ L< 35 mm, and counted the number of malformed specimens in each class. The length of all athyrids were measured by a vernier caliper. All photographs were taken using a Nikon D5100 camera with a Micro-Nikkor 55 mm f3.5 lens.

To explore whether athyrid deformities were caused by environmental factors, trace and

rare earth elements of whole-rock samples from specific levels within the Hongguleleng Formation were measured. Samples BL–1 and BL–2 were obtained from the lower part of the Lower Member of the Hongguleleng Formation, which yielded abundant ~~undeformed~~ athyrids. Samples BL–3 and BL–4 came from the upper part of the Lower Member, form where the ~~deformed~~ fossils described in this paper were obtained. Samples BL–5, BL–6 and BL–7 were collected from the Middle Member of the Hongguleleng Formation; only a few athyrids occurred at the bottom of this member, and the group almost disappeared above that level. Sample B9b–1 was from the Upper Member, which yielded a small number of athyrids. Besides, the trace elements and rare earth elements of four athyrid shells were measured. Samples CL69 and CR178 are ~~undeformed~~ shells, while CLJ13 and CRJ29 are malformed shells. All samples were ground into powder and analyzed in the ALS Minerals/ALS Chemex (Guangzhou) Co. Ltd. Rare earth and trace elements were fused with lithium borate, and quantitatively analyzed by ICP-MS with Elan 9000 Perkin Elmer that was made in America. The Ce_{anom} is equal to $lg[3Ce_n/(2La_n+Nd_n)]$, and Ce_n, La_n and Nd_n were NASC-normalized of Ce, La and Nd, respectively.

Results

Of the 603 athyrid fossils, macroscopic ~~deformities~~ were detected in 57 specimens. The most common teratomorphy is obvious asymmetry on the left and right sides of the shells (Fig. 1B–E, G–J), significantly different from common, ~~undeformed~~ specimens (Fig. 1A, F). Malformation is more obvious on the dorsal valves, and is mainly visible as significantly widening or narrowing on one side of the shell (Fig. 1D1, G1, H1, J1). Near the anterior border

of the dorsal valves, the grooves on both sides of the fold are significantly different from those of undeformed specimens, with some grooves being wider (Fig. 1B1, C1, E1, I1), others being narrower, and some almost disappearing (Fig. 1D1, G1). On the ventral valves, in addition to the unequal size on either side of the shell, the sulcus is slightly curved in some malformed specimens (Fig. 1B2, E2, I2). In frontal view, the asymmetry is more obvious, and is mainly manifested as different depths and widths of the grooves on both sides of the fold (Fig. 1B3–E3, G3–J3); for example, the grooves on one side of some specimens become deeper and wider, up to twice as much as those on the non-deformed side (Fig. 1B3). In addition, the grooves of some specimens become shallower and narrower (Fig. 1H3), even almost disappearing on one side of a few specimens (Fig. 1D3, G3). In the malformed specimens, the commissure on the front of the dorsal and ventral valves forms irregular wavy lines, markedly different from the regular wavy lines in undeformed specimens (Fig. 1A3, F3).

Of the 198 specimens of *Cleiothyridina* and 405 of *Crinisarina*, 18 (9.1%) *Cleiothyridina* and 39 (9.63%) *Crinisarina* were malformed. The overall malformation rate was 9.45%, nearly one-tenth of all specimens (Fig. 2A). In all malformed specimens, the distribution of malformations is asymmetric on the shells in dorsal view, malformations occur in right side of 25 shells of *Crinisarina*, but there are only 14 in left side of shells. For the *Cleiothyridina*, malformation occur in right side of 14 shells, while in left side of 3 shells, and in both sides of one shell (Supplemental file 1). Moreover, malformed individuals occur in almost all size classes (Fig. 2B, C). The malformation percentages of *Crinisarina* are 5.56% (10 mm≤ H< 15 mm), 8.5% (15 mm≤ H< 20 mm), 13.7% (20 mm≤ H< 25 mm) and 11.1% (25 mm≤ H< 30 mm); those

of *Cleiothyridina* are 9.68% (10 mm≤ H< 15 mm), 9.3% (20 mm≤ H< 25 mm) and 14.8% (25 mm≤ H< 30 mm). Thus, shell-malformation occurs at different athyrid growth stages, and the probability of ~~deformity~~ is higher in larger specimens. That indicates a higher probability of ~~deformity~~ during advanced ontogenetic stages of the studied brachiopod taxa.

Discussion

Western Junggar is part of the Central Asian Orogenic Belt (*Buckman & Aitchison, 2004; Windley et al., 2007*). This region experienced strong tectonic activity during the Paleozoic, resulting in different degrees of metamorphism or deformation of the Paleozoic strata in the study area (*Xu et al., 2009; Gong & Zong, 2015; Wang & Zhang, 2019*). Athyrids exhibiting left-right asymmetry might have resulted from tectonic deformation; however, there is no obvious stratal deformation in the Hongguleleng Formation in the Buninuer section. This section has yielded fossils (e.g., trilobites, crinoids, and corals) that are well-preserved in three dimensions (Fig. 3A), which obviously differs from specimens obtained from distorted strata affected by tectonic deformation (Fig. 3B). Moreover, asymmetry was not detected in other brachiopods from the same layer, so the ~~deformed~~ specimens were not affected by the tectonic activity. A very small number of athyrid specimens cracked before lithification of the sediment are also significantly different from these asymmetric specimens, and they can be easily distinguished (Fig. 3D).

Epibionts can cause malformation of their hosts; such phenomena have also been reported for shelly fossils (e.g., *Klug & Korn, 2001; Checa, Okamoto & Keupp, 2002; Zatoń & Borszcz, 2013; Mironenko, 2016; Stilkerich, Smrecak & De Baets, 2017*). Some athyrids from the Upper

Devonian of western Junggar bear epibionts, such as corals and bryozoans. However, epibionts are not found on any malformed specimens; on the contrary, specimens bearing shelled epibionts or epibiont with mineralized shells/skeletons are all ~~undeformed~~ shells (Fig. 3C). Therefore, it is unlikely that these athyrid teratomorphies were caused by epibionts. However, endoparasitic organism cannot be ruled out as a teratogenic factor (e.g., *Savazzi, 1995; Vinn, Wilson & Toom, 2014*), as well as epiparasitic shell-less (soft-bodied) organisms and microorganisms, they are likely to cause ~~deformities~~ in these athyrid shells from western Junggar. For the specific identity of endoparasites, shell-less organisms and microorganisms, it is difficult to confirm because their poor preservation or they are indiscernible in the fossil record. Some malformed brachiopod were caused by predators, which presented the fractures, indentations, and scars on the shells, and often accompanied by repaired signs (e.g., *Alexander, 1986; Kowalewski, Flessa & Marcot, 1997; Happer, 2005; Vinn, 2017*). In these malformed athyrid shells from western Junggar, except for a pair of indentations on the opposite valves of specimen BGEG-CLJ01 (Fig. 3H), no wounds or scars were found on other specimens. Most specimens only showed left-right asymmetry of the shells, reflecting that predation is not the main cause of the malformation, but predators may preyed on the malformed athyrids.

Malformations of organisms may also be related to their living environment. Changes in certain environmental factors, such as oxygen deficiency or excessive organic matter, heavy metals, and toxic elements, often lead to the malformation or even death of organisms. The high number of malformed athyrids from the Upper Devonian strata might be related to the marine environment in western Junggar at that time. Excessive organic matter is a common factor, and

eutrophication has been identified in the Late Devonian sea (*Murphy, Sageman & Hollander, 2000*). *Suttner et al. (2014)* found that there were no significant changes in the total organic carbon (TOC) content through the Lower Member of the Hongguleleng Formation at its type locality, i.e., the TOC content of the beds with ~~deformed~~ specimens was basically the same as that of sediments with only ~~undeformed~~ specimens. *Copper (1967)* studied ~~deformities~~ of the Devonian brachiopod *Kerpina* in the Eifel region, Germany, and concluded that the variations in the shell-morphology resulted from the influence of bottom currents on the immobile *Kerpina*, which had a thick, short pedicle. However, this mechanism cannot be used to explain the ~~deformity~~ of these athyrids in western Junggar, because large numbers of other benthic organisms (i.e., brachiopods, corals, bryozoans, and stromatoporoids), which are all ~~undeformed~~ in the same layer. In addition, the fossils preserved in the upper part of the Lower Member of the Hongguleleng Formation are relatively complete, and there is no evidence of strong bottom currents, so the influence of bottom currents can be excluded as a teratogenic factor. *Hoel (2011)* found the shells of brachiopod *Pentlandina loveni*, from the Sliurian Högklint Formation in Gotland (Sweden), are commonly markedly asymmetric, and some groups of shells occur in tight clusters, each apparently attached to other shells of the same species. He interpreted these asymmetrical shells resulted from the limited space for growth, i.e., overcrowded conditions. However, all specimens from western Junggar are isolated, instead of tight clusters or attached to other shells. Furthermore, if they are living in overcrowded space, the distribution of malformation should be random or almost uniform on both sides of the shells, but the malformations commonly occur on the right side of athyrids shells (dorsal view) from western

Junggar (Supplemental file 1), so the overcrowded conditions also can be excluded.

Marine hypoxia could also lead to brachiopod ~~deformities~~. *He et al. (2017)* for example, proposed that hypoxia was a major factor in the miniaturization of brachiopods during the end-Permian in southern China. U/Th and Ce_{anom} are often used as indicators of marine hypoxia (*Jones & Manning, 1994; Carmichael et al., 2014, 2016*). For the sediments of the Hongguleleng Formation at the Buninuer section, the U/Th ratio of sample BL–4 fell into the oxic range, whereas that of sample BL–3 fell into the dysoxic range; both Ce_{anom} values were near the oxic–anoxic boundary (Fig. 4, Supplemental file 2). However, the uranium enrichment factor (U_{EF}, *Algeo & Liu, 2020*) of above two samples reached 0.69 and 0.19 (in comparison to average limestones, *Wedepohl, 1970*), i.e., the uranium is depleted, and indicating an oxic condition. In addition, a low TOC content (*Suttner et al., 2014*), shallow-marine benthic fossils (e.g., corals, trilobites, brachiopods and echinoderms) occur in abundance in the same horizon together with malformed athyrids (*Liao, 2002*), rich trace fossils reflected not oxygen restricted benthic environment (*Fan & Gong, 2015; Stachacz et al., 2021*), and the beds lack sedimentary indicators of anoxia (such as black shale), also suggest that hypoxia presumably did not occur during deposition of the upper part of the Lower Member of the Hongguleleng Formation.

High levels of heavy metals or toxic elements can also lead to malformation of organisms soft and hard tissue, as has been proven for a large number of living organisms (*Wang, Yang & Wang, 2009; Ma et al., 2011; Zhao et al., 2017; Lasota et al., 2018; Riani, Cordova & Arifin, 2018*). For example, when Cu and Zn were added to the water for feeding the foraminiferan *Ammonia beccarii*, the organisms developed ~~deformities~~ (*Sharifi, Croudace & Austin, 1991*), and

when scallops were placed in wastewater from a gold mine with concentrations of 14% and 50% for 6 h, the ~~deformity rate~~ increased by 6% and 21%, respectively (*Ma et al., 2011*). Sediments have been demonstrated to be an important source of heavy metals for benthic animals (*Wang, Stupakoff & Fisher, 1999*). The levels of heavy metals and toxic elements through the Hongguleleng Formation are presented in Fig. 4 and Supplemental file 2. The levels of some heavy metals (e.g., cadmium, lead, barium, and zinc) in the layer with the malformed athyrid shells are relatively high compared to the levels in the lower part of the Lower Member, particularly cadmium and lead. The levels of cadmium are 0.02 and 0.03 ppm in the lower part of the Lower Member, and are 0.03 and 0.04 ppm in the horizon that yielded the ~~deformed~~ fossils. The lead contents are 1.3 and 2.2 ppm in the lower part, but 5.1 and 5.2 ppm in the upper part. In the Middle Member of the Hongguleleng Formation, where athyrids almost disappeared, the heavy metal levels are even higher. In the Upper Member, where athyrids reappear, the heavy-metal content decreases again (Fig. 4). Thus, the abundance of athyrids is negatively correlated with the levels of heavy metals, but the number of malformed specimens is positively correlated with that, especially that of lead (Fig. 4). Furthermore, the levels of most heavy metals and toxic elements are slightly higher in malformed shells than in ~~undeformed~~ shells, particularly lead, silver, cobalt and arsenic (Supplemental file 3). In the studied specimens of teratomorphic *Cleiothyridina* and *Crinisarina*, the lead, silver, cobalt, and arsenic levels were all higher than those of ~~undeformed~~ shells. In *Cleiothyridina* the levels of lead, silver, cobalt, and arsenic were 2.3, 0.01, 2.0, and 2.9 ppm, respectively, in ~~undeformed~~ shells, but 2.6, 0.03, 2.5, and 3.6 ppm, respectively, in malformed shells. In *Crinisarina*, the levels of lead, silver, cobalt, and arsenic in

~~undeformed~~ shells were 1.9, <0.01, 2.6, and 2.2 ppm, respectively, whereas in the ~~deformed~~ specimens, the levels were 7.2, 0.01, 3.2, and 2.5 ppm, respectively (Supplemental file 3). However, the contents of cobalt and other heavy metals (i.e., copper, chromium, and vanadium) did not change significantly in the sediments from the ~~undeformed~~ athyrids-bearing layers to the layers containing malformed specimens, and the contents of arsenic and silver even decreased in the layers containing malformed athyrids (Fig. 4). Therefore, these heavy metals or toxic elements in greater concentrations may not be related to the ~~deformity~~ of athyrids. Only the lead content in sediments is positively correlated with the athyrid shell ~~deformation~~, but negatively correlated with the abundance, while the lead content of malformed shells is higher than that of ~~undeformed~~ shells.

Lead is a common type of marine heavy-metal, and excessive lead content in the sea often leads to malformation or even death of shellfish, or at least affects their growth (*Li, Sun & Li, 2011*). In Upper Devonian strata of western Junggar, the ~~deformity rate~~ of athyrids is nearly one in ten. In addition, the heavy metal (especially lead) content in sediments is higher than that of sediments containing only ~~undeformed~~ shells, and the levels of some heavy metals are higher in ~~deformed~~ shells than in ~~undeformed~~ shells. However, the difference of lead concent in the shells and surrounding rocks of ~~undeformed~~ and malformed brachiopods is still within the same order of magnitude, and no ~~deformities~~ have been found in other brachiopods taxa except these two genera. Therefore, it is not entirely certain that slightly higher lead content could cause ~~deformities~~ in these athyrid shells. In the future, geochemical analysis of more athyrid shells with novel state-of-the art methods and a comprehensive comparison of heavy metal content from

adjacent horizons and other brachiopods may be able to provide further testing of the link between these ~~deformities~~ and environmental factors.

Conclusions

Some specimens of two athyrid genera, *Cleiothyridina* and *Crinisarina*, from the Upper Devonian Hongguleleng Formation in western Junggar are obviously deformed, mainly in the form of asymmetry of the left and right sides of the shells. The ~~deformity rate~~ is nearly 10% of specimens. Malformation is apparent in individuals of different sizes, with larger individuals being more likely to exhibit malformation. Based on the study of the burial state and preserved environment of the fossils, and geochemical analysis of the sediments and athyrid shells and comparison with rock material from horizons that did not contain teratomorphic specimens, we hypothesize that the ~~deformities~~ were possibly caused by unidentified (?soft-bodied) epi/endoparasites, or a low probability, that slightly high heavy-metal (specifically lead) in the sea, rather than eutrophication, bottom current activity, overcrowded conditions, hypoxia or other factors.

Acknowledgements

We would like to thank Zhen Shen, Chao Guo and Junyan Dong, all from China University of Geosciences (Wuhan) for their help in the field work. We appreciate much the constructive and critical comments from Thomas Suttner, Uwe Balthasar, Michał Rakociński, two anonymous reviewers and Editor Kenneth De Baets, which aided in the further improvement of the manuscript.

References

285 **Alexander RR. 1986.** Resistance to and repair of shell breakage induced by durophages in Late
286 Ordovician brachiopods. *Journal of Paleontology* **60:** 273–285
287 DOI10.1017/s0022336000021806.
288 **Algeo TJ, Liu JS. 2020.** A re-assessment of elemental proxies for paleoredox analysis.
289 *Chemical Geology* **540:** 119549. DOI 10.1016/j.chemgeo.2020.119549
290 **Babcock LE. 1993.** Trilobite malformations and the fossil record of behavioral asymmetry.
291 *Journal of Paleontology* **67:** 217–229 DOI 10.1017/S0022336000032145.
292 **Ballent SC, Carignano AP. 2008.** Morphological abnormalities in Late Cretaceous and early
293 Paleocene foraminifer tests (northern Patagonia, Argentina). *Marine Micropaleontology* **67:**
294 288–296 DOI 10.1016/j.marmicro.2008.02.003.
295 **Bralower TJ, Self-Trail JM. 2016.** Nannoplankton malformation during the Paleocene–Eocene
296 Thermal Maximum and its paleoecological and paleoceanographic significance.
297 *Paleoceanography* **31:** 1423–1439. DOI 10.1002/2016PA002980.
298 **Buckman S, Aitchison JC. 2004.** Tectonic evolution of Palaeozoic terranes in West Junggar,
299 Xinjiang, northwest China. In: Malpas J, Fletcher CJ, Aitchison JC, Ali J (Eds.) Aspects of
300 the Tectonic Evolution of China. *Geological Society, London, Special Publications*
301 **226:**101–129.
302 **Buffetaut E, Li JJ, Tong HY, Zhang H. 2007.** A two-headed reptile from the Cretaceous of
303 China. *Biology Letters* **3:** 80–81 DOI 10.1098/rsbl.2006.0580.
304 **Carmichael SK, Waters JA, Batchelor CJ, Coleman DM, Suttner TJ, Kido E, Moore LM,**
305 **Chadimová L. 2016.** Climate instability and tipping points in the Late Devonian: Detection

306 of the Hangenberg Event in an open oceanic island arc in the Central Asian Orogenic Belt.
307 *Gondwana Research* **32:** 213–231 DOI 10.1016/j.gr.2015.02.009350

308 **Carmichael SK, Waters JA, Suttner TJ, Kido E, Dereuil AA. 2014.** A new model for the
309 Kellwasser Anoxia Events (Late Devonian): Shallow water anoxia in an open oceanic
310 setting in the Central Asian Orogenic Belt. *Palaeogeography, Palaeoclimatology,*
311 *Palaeoecology* **399:** 394–403 DOI 10.1016/j.palaeo.2014.02.016.

312 **Checa AG, Okamoto T, Keupp H. 2002.** Abnormalities as natural experiments: a
313 morphogenetic model for coiling regulation in planispiral ammonites. *Paleobiology* **28:**
314 127–138.

315 **Copper P. 1967.** Morphology and distribution of *Kerpina* Struve (Devonian Atrypida).
316 *Paläontologische Zeitschrift* **41:** 73–85 DOI 10.1007/BF02998550.

317 **De Baets K, Hoffmann R, Mironenko A. 2021.** Evolutionary history of cephalopod pathologies
318 linked with parasitism. In: De Baets K, Huntley JW, eds. The Evolution and Fossil Record
319 of Parasitism. *Topics in Geobiology* **50:** Springer, Cham, 203–249.

320 **De Baets K, Huntley JW, Klompmaker AA, Schiffbauer JD, Muscente AD. 2021.** The fossil
321 record of parasitism: Its extent and taphonomic constraints. In: De Baets K, Huntley JW,
322 eds. The Evolution and Fossil Record of Parasitism. *Topics in Geobiology* **50:** Springer,
323 Cham, 1–50.

324 **De Baets K, Keupp H, Klug C. 2015.** Parasites of ammonoids. In: Klug C, Korn D, De Baets K,
325 Kruta I, Mapes RH, eds. Ammonoid Paleobiology: From anatomy to ecology. *Topics in*
326 *Geobiology* **43:** Springer, Dordrecht, 837–875.

Fan RY, Gong YM. 2016. Ichnological and sedimentological features of the Hongguleleng Formation (Devonian–Carboniferous transition) from the western Junggar, NW China. *Palaeogeography, Palaeoclimatology, Palaeoecology* **448:** 207–223 DOI 10.1016/j.palaeo.2015.12.009.

Gong YM, Zong RW. 2015. Paleozoic stratigraphic regionalization and paleogeographic evolution in western Junggar, Northwestern China. *Earth Science—Journal of China University of Geosciences* **40:** 461–484.

Han NR, Chen X. 1994. Regeneration in *Cardiograptus*. *Lethaia* **27:** 117–118.

Happer EM. 2005. Evidence of predation damage in pliocene *Apletosia maxima* (brachiopoda). *Palaeontology* **48:** 197–208 DOI 10.1111/j.1475-4983.2004.00433.x.

He WH, Shi GR, Xiao YF, Zhang KX, Yang TL, Wu HT, Zhang Y, Chen B, Yue ML, Shen J, Wang YB, Yang H, Wu SB. 2017. Body-size changes of latest Permian brachiopods in varied palaeogeographic settings in South China and implications for controls on animal miniaturization in a highly stressed marine ecosystem. *Palaeogeography, Palaeoclimatology, Palaeoecology* **486:** 33–45 DOI 10.1016/j.palaeo.2017.02.024.

Hoel OA. 2011. Strophomenidae, Leptostrophiidae, Strophodontidae and Shaleriidae (Brachiopoda, Strophomenida) from the Silurian of Gotland, Sweden. *Paläontologische Zeitschrift* **85:** 201–229. DOI 10.1007/s12542-010-0088-3.

Hoffmann R, Keupp H. 2015. Ammonoid paleopathology. In: Klug C, Korn D, De Baets K, Kruta I, Mapes RH, eds. Ammonoid Paleobiology: From anatomy to ecology. *Topics in Geobiology* **43:** Springer, Dordrecht, 877–926

348 **Hou HF, Lane NG, Waters JA, Maples CR. 1993.** Discovery of a new Famennian echinoderm
349 fauna from the Hongguleleng Formation of Xinjiang, with redefinition of the formation.
350 *Stratigraphy and Paleontology of China* **2:** 1–18.
351 **Itano WM. 2013.** Abnormal serration rows on a tooth of the Pennsylvanian chondrichthyan
352 edestus. In: Lucas SG, DiMichele WA, Barrick JE, Schneider JW, Spielmann JA, eds. *The*
353 *Carboniferous–Permian Transition*. New Mexico Museum of Natural History and Science,
354 Bulletin **60:** 139–142.
355 **Jones B, Manning DAC. 1994.** Comparison of geochemical indices used for the interpretation
356 of palaeoredox conditions in ancient mudstones. *Chemical Geology* **111:** 111–129. DOI
357 10.1016/0009-2541(94)90085-X.
358 **Kelley PH, Kowalewski M, Hansen TA. 2003.** *Predator-prey interactions in the fossil record*.
359 Kluwer Academic/Plenum Publishers. New York, Boston, Dordrecht, London, Moscow.
360 **Klug C, Korn D. 2001.** Epizoa and post-mortem epicoles on cephalopod shells–Devonian and
361 Carboniferous examples from Morocco. *Berliner geowissenschaftliche Abhandlungen E* **36:**
362 145-155.
363 **Kowalewski M, Flessa KW, Marcot JD. 1997.** Predatory scars in the shells of a recent lingulid
364 brachiopod: paleontological and ecological implications. *Acta Palaeontologica Polonica* **42:**
365 497–532.
366 **Lasota R, Gierszewska K, Viard F, Wolowicz M, Dobrzyn K, Comtet T.**
367 **2018.** Abnormalities in bivalve larvae from the Puck Bay (Gulf of Gdansk, southern Baltic
368 Sea) as an indicator of environmental pollution. *Marine Pollution Bulletin* **126:** 363–371

DOI 10.1016/j.marpolbul.2017.11.015.

Li H, Sun HS, Li L. 2011. Effects of lead pollution on marine organisms: a review. *Fisheries Science* **30:** 177–181.

Liao WH. 2002. Biotic recovery from the Late Devonian F–F mass extinction event in China. *Science in China, Series D* **45:** 380–384. DOI 10.1360/02yd9039.

Lindström A, Peel JS. 2010. Shell repair and shell form in Jurassic pleurotomarioid gastropods from England. *Bulletin of Geosciences* **85:** 541–550 DOI 10.3140/bull.geosci.1205.

Ma JX, Zhang YK, Song XK, Liu AY, Ren LH, Wang WJ. 2011. Research progress of heavy metals stress on the shellfish toxicity. *Transactions of Oceanology and Limnology* **2:** 35–42.

Ma XP, Zhang MQ, Zong P, Zhang YB, Lü D. 2017. Temporal and spatial distribution of the Late Devonian (Famennian) strata in the northwestern border of the Junggar Basin, Xinjiang, Northwestern China. *Acta Geologica Sinica (English Edition)* **91:** 1413–1437 DOI 10.1111/1755-6724.13370.

Mironenko AA. 2016. A new type of shell malformation caused by epizoans in Late Jurassic ammonites from Central Russia. *Acta Palaeontologica Polonica* **61:** 645–660 DOI 10.4202/app.00100.2014.

Morris SC. 1981. Parasites and the fossil record. *Parasitology* **82:** 489–509. DOI 10.1017/S0031182000067020

Murphy AE, Sageman BB, Hollander DJ. 2000. Eutrophication by decoupling of the marine biological cycles of C, N, and P: A mechanism for the Late Devonian mass extinction. *Geology* **28:** 427–430. DOI 10.1130/0091-7613(2000)28<427:EBDOTM>2.0.CO;2.

Owen AW. 1985. Trilobite abnormalities. *Transactions of the Royal Society of Edinburgh* **76:** 255–272 DOI 10.1017/S0263593300010488.

Rouse GW. 2005. Fossil parasites. In: Rohde K, ed. *Marine Parasitology*. CABI Publishing, Oxon, 172–174.

Riani E, Cordova MR, Arifin Z. 2018. Heavy metal pollution and its relation to the malformation of green mussels cultured in Muara Kamal waters, Jakarta Bay, Indonesia. *Marine Pollution Bulletin* **133:** 664–670 DOI 10.1016/j.marpolbul.2018.06.029.

Savazzi E. 1995. Parasite-induced teratologies in the Pliocene bivalve Isognomon Maxillatus. *Palaeogeography, Palaeoclimatology, Palaeoecology* **116:** 131–139 DOI 10.1016/0031-0182(94)00097-R.

Sharifi AR, Croudace IW, Austin RL. 1991. Benthic foraminiferids as pollution indicators in Southampton Water, southern England, U.K. *Journal of Micropalaeontology* **10:** 109–113. DOI 10.1144/jm.10.1.109.

Shen Z, Steemans P, Gong YM, Zong RW, Servais T. 2021. Palynological analysis of the lower member of the Hongguleleng Formation and discussion of the Frasnian/Famennian boundary in Western Junggar, NW China. *Review of Palaeobotany and Palynology* **295:** 104504. DOI /10.1016/j.revpalbo.2021.104504

Stachacz M, Kondas M, Filipiak P, Ma XP. 2021. Environment and age of the Upper Devonian–Carboniferous Zhulumute and Hongguleleng Formations (Junggar Basin, NW China): Ichnological and palynological aspects. *Acta Geologica Sinica (English Edition)* **95:** 724–739. DOI 10.1111/1755-6724.14408.

411 **Stilkerich J, Smrecak TA, De Baets K. 2017.** 3D-Analysis of a non-planispiral ammonoid from the
412 Hunsrück Slate: natural or pathological variation? *PeerJ* **5:** e3526. DOI 10.7717/peerj.3526.
413 **Suttner TJ, Kido E, Chen XQ, Mason R, Waters JA, Fryda J, Mathieson D, Molloy PD,**
414 **Pickett J, Webster GD, Frydová B. 2014.** Stratigraphy and facies development of the
415 marine Late Devonian near the Boulongour Reservoir,northwest Xinjiang,China. *Journal of*
416 *Asian Earth Sciences* **80:** 101–118. DOI 10.1016/j.jseaes.2013.11.001.
417 **Thomka JR, Malgieri TJ, Brett CE. 2014.** A swollen crinoid pluricolumnal from the Upper
418 Ordovician of northern Kentucky, USA: the oldest record of an amorphous paleopathologic
419 response in Crinoidea? *Estonian Journal of Earth Sciences* **63:** 317–322 DOI
420 10.3176/earth.2014.37.
421 **Tougard C, Ducrocq S. 1999.** Abnormal fossil upper molar of Pongo from Thailand:
422 Quaternary climatic changes in southeast Asia as a possible cause. *International Journal of*
423 *Primatology* **20:** 599–607. DOI 10.1023/A:1020346908618.
424 **Vandenbroucke TRA, Emsbo P, Munnecke A, Nuns N, Duponchel L, Lepot K, Quijada M,**
425 **Paris F, Servais T, Kiessling W. 2015.** Metal-induced malformations in early Palaeozoic
426 plankton are harbingers of mass extinction. *Nature Communications* **6:** 7966 DOI
427 10.1038/ncomms8966.
428 **Vinn O. 2017.** Predation in the Ordovician and Silurian of Baltica. *Historical Biology* **29:** 11–16
429 DOI 10.1080/08912963.2015.1092964.
430 **Vinn O. 2018.** Traces of predation in the Cambrian. *Historical Biology* **30:** 1043–1049 DOI
431 10.1080/08912963.2017.1329305.

Vinn O, Wilson MA, Toom U. 2014. Earliest rhynchonelliform brachiopod parasite from the Late Ordovician of northern Estonia (Baltica). *Palaeogeography, Palaeoclimatology, Palaeoecology* **411:** 42–45 DOI 10.1016/j.palaeo.2014.06.028.

Vršanský P, Liang JH, Ren D. 2012. Malformed cockroach (Blattida: Liberiblattinidae) in the Middle Jurassic sediments from China. *Oriental Insects* **46:** 12–18 DOI 10.1080/00305316.2012.675482.

Wang GC, Zhang P. 2019. Emplacement of ophiolitic mélanges and its tectonic significance: insights from the structural analysis of the remnant oceanic basin-type ophiolitic mélanges**.** *Earth Science* **44:** 1688-1704 DOI 10.3799/dqkx.2019.056.

Wang WX, Stupakoff I, Fisher NS. 1999. Bioavailabitity of dissolved and sediment-bound metals to a marine deposit-feeding polychaete. *Marine Ecology Progress Series* **178:** 281–293. DOI 10.3354/meps178281.

Wang XY, Yang HS, Wang Q. 2009. Ecotoxicological effects of heavy metal pollution on bivalves: a review. *Marine Sciences* **33:** 112–118.

Weddige K. 1990. Pathological Conodonts. *Courier Forschungsinstitut Senckenberg* **118:** 563–589.

Wedepohl KH. 1970. Geochemische Daten von sedimentären Karbonaten und Karbonatgesteinen in ihrem faziellen und petrogenetischen Aussagewert. *Verhandlungen der Geologischen Bundesanstalt* **4:** 692–705.

Windley BF, Alexeiev D, Xiao WJ, Kröner A, Badarch G. 2007. Tectonic models for accretion of the Central Asian Orogenic Belt. *Journal of Geological Society, London* **164:** 31–47 DOI 10.1144/0016-76492006-022.

Witzmann F, Rothschild BM, Hampe O, Sobral G, Gubin YM, Asbach P. 2013. Congenital Malformations of the Vertebral Column in Ancient Amphibians. *Anantomia Histologia Embryologia* **43:** 90–102 DOI 10.1111/ahe.12050.

Xu QQ, Ji JQ, Gong JF, Zhao L, Tu JY, Sun DX, Tao T, Zhu ZH, He GQ, Hou JJ. 2009. Structural style and deformation sequence of western Junggar, Xinjiang, since Late Paleozoic. *Acta Petrologica Sinica* **25:** 636–644.

Zatoń M, Borszcz T. 2013. Encrustation patterns on post-extinction early Famennian (Late Devonian) brachiopods from Russia. *Historical Biology* **25:** 1–12. DOI 10.1080/08912963.2012.658387.

Zhao XH, Fan C, Zhao S, Wang LZ, Gui, F. 2017. Advances in the study on the benthic foraminiferal response to marine heavy metal pollution. *Acta Micropalaeontologica Sinica* **34:** 440–446.

Zong P, Ma XP. 2018. Spiriferide brachiopods from the Famennian (Late Devonian) Hongguleleng Formation of western Junggar, Xinjiang, northwestern China. *Palaeoworld* **27:** 66–89. DOI 10.1016/j.palwor.2017.07.002.

Zong P, Ma XP, Xue JZ, Jin XC. 2016. Comparative study of Late Devonian (Famennian) brachiopod assemblages, sea level changes, and geo-events in northwestern and southern China. *Palaeogeography, Palaeoclimatology, Palaeoecology* **448:** 298–316. DOI

10.1016/j.palaeo.2015.11.024.

Zong RW, Wang ZH, Fan RY, Song JJ, Zhang XS, Shen Z, Gong YM. 2020. New knowledge on the Hongguleleng Formation and Devonian–Carboniferous boundary in western Junggar, Xinjiang. *Acta Geologica Sinica* **94:** 2460–2475.

Figure 1

Athyrids from the upper part of the Lower Member of the Hongguleleng Formation (Upper Devonian) in western Junggar

(A–E) *Crinisarina*, figure (A) (specimen number BGEG-CR324) is a ~~undeformed~~ specimen; figures (B–E) (specimen numbers BGEG-CRJ05, BGEG-CRJ10, BGEG-CRJ18 and BGEG-CRJ17) are malformed specimens, with malformations indicated by white arrows. (F–J) *Cleiothyridina*, figure (F) (specimen number BGEG-CL98) is a ~~undeformed~~ specimen; figures (G–J) (specimen numbers BGEG-CLJ06, BGEG-CLJ01, BGEG-CLJ15 and BGEG-CLJ13) are malformed specimens, with malformations indicated by white arrows. All scales are 10 mm.

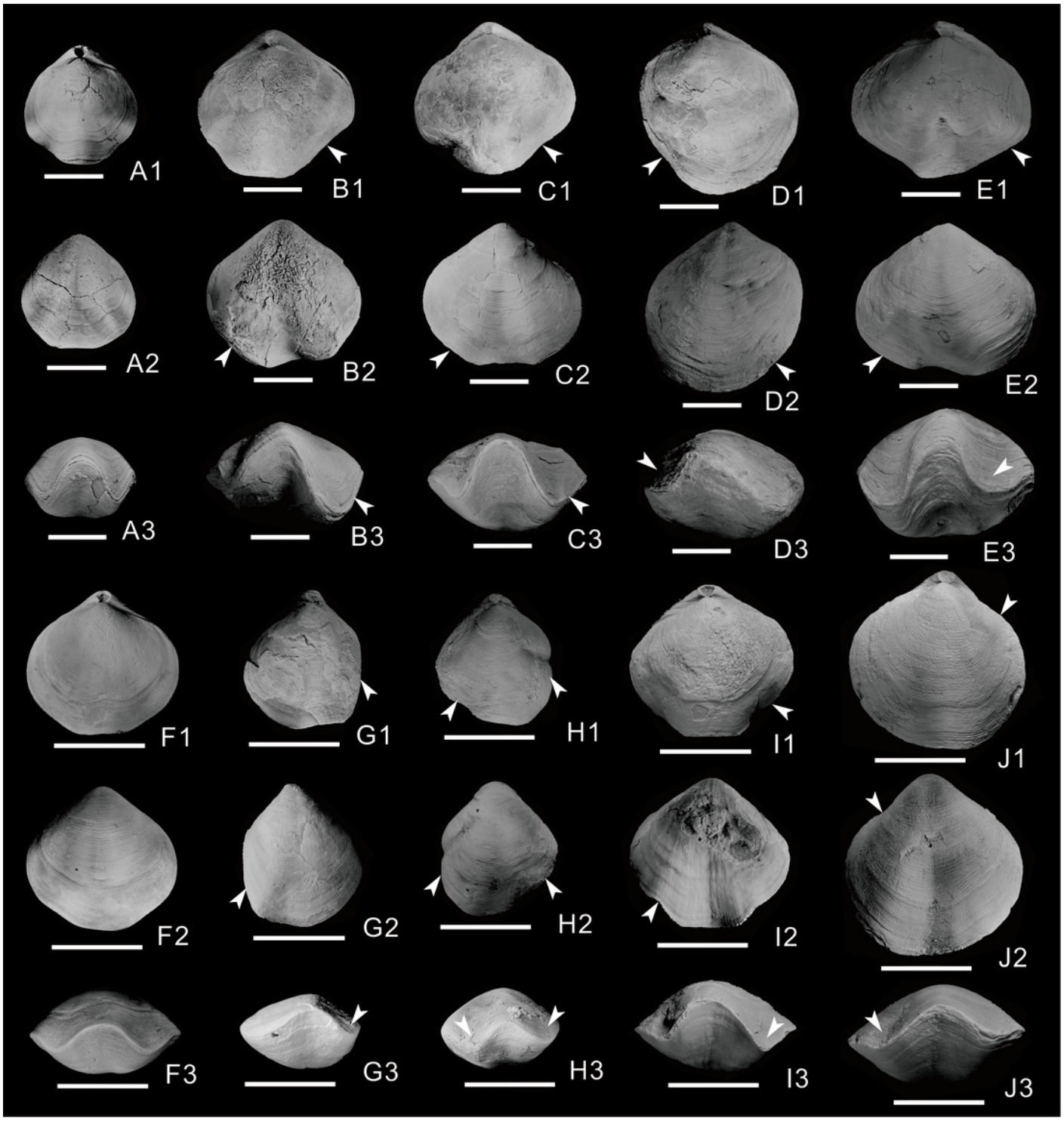
A1
B1
C1
D1
E1
A2
B2
C2
D2
E2
A3
B3
C3
D3
E3
F1
G1
H1
I1
J1
F2
G2
H2
I2
J2
F3
G3
H3
I3
J3

Figure 2

Histogram showing the number of malformed athyrids (A) and the distribution of ~~undeformed~~ and malformed specimens in different size classes (B–C) from the Upper Devonian Hongguleleng Formation in western Junggar

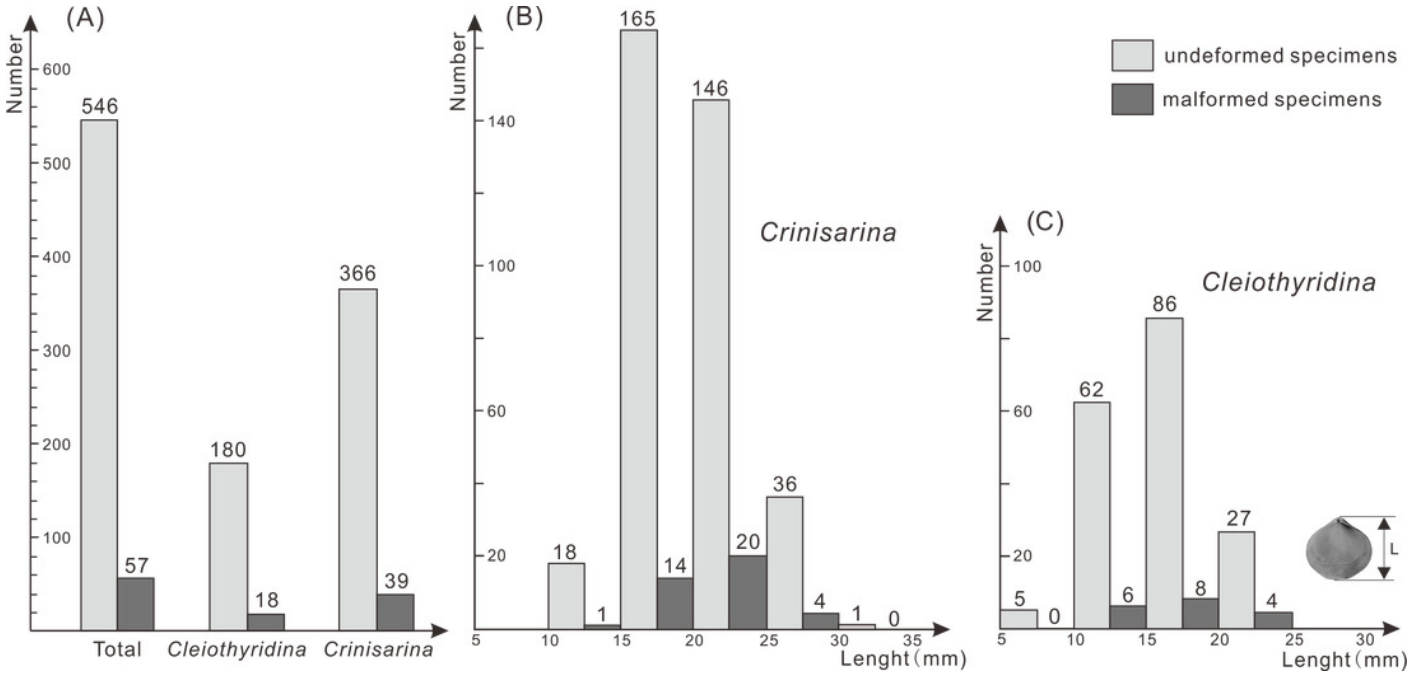

Figure 3

Some crinoid stems and athyrids from western Junggar

(A) Three-dimensional crinoid stem preserved in muddy limestone from the upper part of the Lower Member of the Hongguleleng Formation in the Buninuer section; (B) flattened crinoid stem preserved in the calcareous siltstone distorted by tectonic activity, Carboniferous Hala'alate Formation, western Junggar; (C) coral parasitizing a ~~undeformed~~ shell of *Crinisarina* (specimen number BGEG-CR44) from the Lower Member of the Hongguleleng Formation; (D) *Cleiothyridina* (specimen number BGEG-CL56) cracked before lithification of the sediment, obviously different from the malformed specimens. All scales are 10 mm.

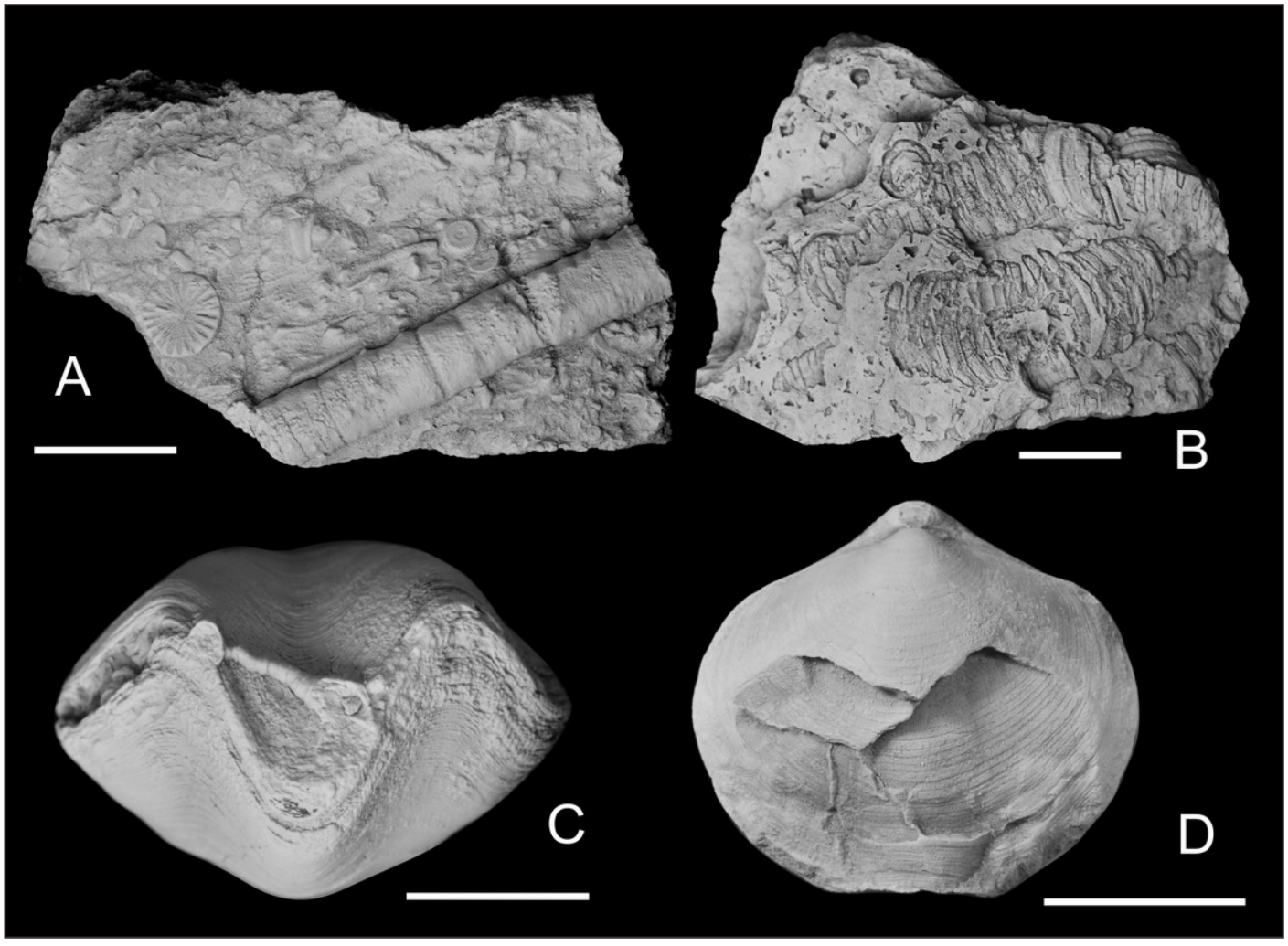

Figure 4

U/Th ratio, Ce_{anom} and distribution of heavy metals and toxic elements in whole rocks in the Upper Devonian Hongguleleng Formation in western Junggar